Localization of blood vessels in in-vitro LSCI images with K-means

F. Lopez-Tiro, H. Peregrina-Barreto, J. Rangel-Magdaleno, J. C. Ramirez-San-Juan
Instituto Nacional de Astrofísica, Óptica y Electrónica
Luis Enrique Erro 1, Santa Maria Tonantzintla, 72840. Puebla, México
Corresponding author: hperegrina@inaoep.mx

***Abstract*— The visualization and localization of blood vessels in Laser Speckle Contrast Imaging is an important task in biomedical applications such as dermatology, neurosciences, and ophthalmology, as it allows to determine the presence of blood vessels and also to estimate properties such as blood flow. This work establishes a review of visualization methods for contrast calculation and improvement in Laser Speckle Contrast Imaging. In addition, it is presented the localization of blood vessels in an automatic way through clustering. The results suggest that the localization of blood vessels depends largely on the calculation and improvement of contrast. If the blood vessel and biological tissue regions are well separated from each other, and the noise level is low, K-means clustering is a powerful tool for locating blood vessels in Laser Speckle Contrast Imaging.**

Keywords: Laser Speckle Contrast Imaging, Localization of blood vessels, K-means clustering.

I. INTRODUCTION

Visualization of blood vessels is an important task in biomedical applications related to blood flow in organs such as the retina [1], brain [2], and skin [3]. Laser Speckle Imaging (LSI) is the most widely used non-invasive technique for measuring blood flow [4].

Speckle is a scattering phenomenon and occurs when photons from a coherent light laser interact with a rough surface such as a biological tissue. The photons that scattering out of the biological tissue are integrated using a LSI acquisition system, producing raw speckle images (RSI images). The movement of red blood cells inside the biological tissue produces a blurred effect in the RSI images. The analysis of the blurring effect is the main interest of LSI [5] for visualize and localize blood vessels. The main limitation of LSI is related to noise. As the blood vessel increases its depth inside the biological tissue, the noise increases too and causes that the blurring effect to decrease, and as a result the visualization of the blood vessel is low. Fortunately, this limitation has been addressed in different ways, with contrast being the most commonly method used representation to improve the blood vessel visualization [6]–[8].

The contrast in RSI images can be determined using traditional methods such as temporal, spatial, and spatial-temporal contrast [9]–[12]. However, contrast images have some drawbacks when the blood vessel is deep, or has a high amount of noise. One of these drawbacks is the fusion of the blood vessels and biological tissue in the contrast image. So contrast improvement methods [13]–[22] seek to attenuate the noise in the contrast images and separate the blood vessel and biological tissue avoiding the merger of regions. Adequate separation of the regions is an objective indicator in improving the visualization of blood vessels. If the separation of these two regions is large (also has a low amount of noise), it is possible to to determine the boundaries of the blood vessel accurately (regardless of depth) in a segmented image.

In this work, two objectives are established. First, to provide a method of automatically locating blood vessels in *in-vitro* contrast images. Second, to perform an objective comparison of the segmentation results in *in-vitro* blood vessels using different contrast computation methods, and thus establish the limitations of the K-means clustering method in contrast images.

II. MATERIALS AND METHODS

A. Dataset

The dataset used in this work contains 126 RSI packages, each package containing 30 RSI images (a standard number in LSI) of straight blood vessels acquired *in-vitro*. The experimental arrangement used to acquire these images consists of a He-Ne Laser ($632.8nm$) which homogeneously illuminates a skin phantom using an optical diffuser (*ModelED1 - C20, Thorlabs Inc*) as shown in Fig. 1b.

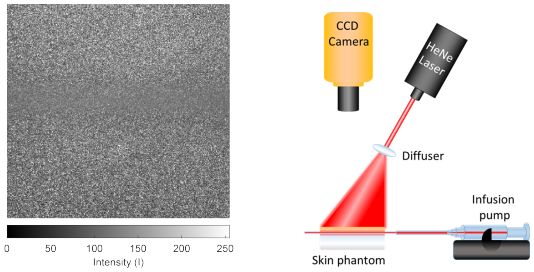

(a) (b)

Fig. 1: (a) RSI image of a *in-vitro* straight blood vessel at $0\mu m$ depth, the central blurring pattern corresponds to the blood vessel, (b) experimental setup that acquires the images of (a).

A package of RSI images is acquired by a CCD camera (*ModelRetiga2000R, QImaging, Canada*) equipped with a macro lens. The skin phantom was manufactured with optical properties (scattering coefficient) similar to human skin, as reported in [23]. Two phantoms were used: one for the epidermis and one for the dermis. Different epidermis layer thicknesses from $0\mu m$ to $1000\mu m$ were used. To simulate the blood vessels of the skin phantom, was used a straight glass capillary with an inside diameter of $700\mu m$ (*thinXXS Microtechnology AG, Germany*) located on the surface of the dermis. The infusion of intralipids at 3% in water was used to simulate the scattering properties of human blood and pumped through the capillaries with a pump (*Model NE-500, NewEraPumpSystemInc*), controlled the blood flow.

The dataset contains 27, 15, 42, 15, and 27 RSI image packages with $0\mu m$, $190\mu m$, $310\mu m$, $510\mu m$, and $1000\mu m$ depth, respectively. The dimensions of the *in-vitro* images for straight blood vessels are 640×480 pixels. The exposure time of the blood vessels is denoted as T. The dataset has T values between $70.60ms$ and $32789.80ms$. The ground truth (GT) was obtained by labeling the blood vessel to a depth of $0\mu m$. The labeling is a binary image consisting of two classes 0 y 1, biological tissue and blood vessel, respectively.

B. Contrast

Laser Speckle Contrast Imaging (LSCI) is the most widely used method to improve the visualization of blood vessels. When an RSI image is computed using a contrast method, a contrasted image (LSCI image) is obtained. Various approaches have been used to calculate (K), defined as the ratio of the standard deviation σ(W) to the average intensity μ(W), where W is an analysis window that moves through the RSI image centered on the x and y coordinates. By definition the values of K are in a range between 0 and 1 [9].

$$K_{x,y} = \frac{\sigma(W)}{\bar{I}(W)} \tag{1}$$

When the elements of W are different from each other, the K value is high or close to 1. In LSCI images, a K value is highly associated with the region of the biological tissue. While a low K value or close to 0 corresponds to the region of the blood vessel, where the elements of W are similar.

C. Tested Contrast Methods

Six contrast methods were implemented because of their performance with small datasets (100 $<$ samples) of *in-vitro* RSI images. These methods can be divided into two important groups: classical contrast calculation methods, and contrast improvement methods.

In the classical contrast methods were tested spatial contrast (*sK*), spatial contrast averaged (sK_{avg}) and space-directional contrast (*sdK*). These methods process RSI images using isotropic and anisotropic analysis windows. On the other hand, contrast improvement methods use some representation of the LSCI images and through non-spatial filtering methods, these methods improve the visualization of the blood vessels (even when they are deep). The contrast improvement methods implemented in this work include Gaussian Sliding Window (GSW) [22], Principal Component Analysis (PCA) [16], and Wavelet Approach (WA) [20].

1) Spatial Contrast (sK): One of the K calculation methods used in this work is *sK*. The *sK* method attenuates the noise considering the neighborhood information of a square and isotropic window ($W^{sK}_{d\times d}$) where d is the size of the window. In Fig. 2 is shown the calculation of K with the window W for an RSI image.

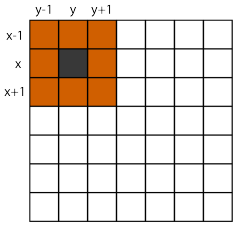

Fig. 2: Pixels used to calculate contrast with an analysis window $d = 3$ for spatial contrast. The orange squares are part of the analysis window, the black square represents the central pixel.

Setting the optimal W size is a problem. In the work [14], establish a methodology to select the optimal size of W. Thus, in this work the size of W is 7 for each RSI image package and all the methods that compute K. The number of LSCI images obtained with *sK* is equal to the number of frames in the LSI package.

2) Spatial Contrast Averaged (sK_{avg}): Another method of calculating K and is inspired by *sK*. sK_{avg} calculates the average of a set of N spatial LSCI images (1) for each pixel located in the coordinates x and y as shown in (2):

$$sK_{avg}(x,y) = \frac{1}{N}\sum_{i=1}^{N} sK(x,y)(i) \tag{2}$$

sK_{avg} maintains a high spatial resolution of K values at the cost of the temporal resolution improving the blood vessel visualization. In terms of dimensionality, the number of LSCI images obtained with sK_{avg} is 1, independent of the number of frames in the RSI image package. In this work, the number of N frames is 30, since it is a standard in LSI.

3) Space-directional contrast (sdK): The last calculation method, K, differs in the shape of the analysis window. In the work [10] proposes *sdK* and calculates K with $1 \times d$ anisotropic windows in four directions. It uses the variance of the directions as a selection criterion for W. The number of LSCI images obtained with *sdK* is equal to the number of frames in the RSI package.

Although *sK*, sK_{avg}, and *sdK* methods are efficient in attenuating superficial blood vessels ($\rho < 100\mu m$), they have drawbacks when depth increases, e.g., they maintain a high amount of noise and it is difficult to establish the boundaries between the blood vessel and biological tissue. To improve the visualization of superficial and deep blood vessels, where the amount of noise is high and the contrast between both regions decreases, contrast improvement methods have been developed. The main objective of these methods is to attenuate the noise present in LSCI images through different filtering techniques.

4) Gaussian Sliding Window (GSW): *GSW* is a method that proposes linear filtering through a Gaussian function. *GSW* attenuates the variations in which traditional methods are inefficient. The parameters used in this algorithm are described in [22]. The number of LSCI images obtained with *GSW* is equal to the number of frames in the RSI package.

5) Principal Component Analysis (PCA): PCA seeks the best projection in terms of least squares. The results presented suggest that reducing dimensionality with PCA improves contrast in both regions and allows for visualization of deep blood vessels up to $1000\mu m$. The parameters selected for this model are described in [16]. In terms of dimensionality, the number of LSCI images obtained with PCA is 1, independent of the number of frames in the RSI image package.

6) Wavelet Approach (WA): WA proposes noise attenuation through a filter bank defined by the Discrete Wavelet Transform. The selection of parameters for the decay process, wavelet function, and filter level are described in [20]. The WA results suggest that attenuating the noise in the blood vessel allows improving the contrast by up to $500\mu m$. In terms of dimensionality, the number of LSCI images obtained with sK_{avg} is 1, independent of the number of frames in the RSI image package.

D. K-means clustering

K-means clustering is a type of unsupervised learning. The clustering method is used when the input data set lacks labels. The objective of this algorithm is to find groups of data. The data points are grouped according to the similarity of characteristics and defined as:

$$C_k = \sum_{a=1}^{k}\sum_{b=1}^{n} \|p_b^{(a)} - c_a\|^2 \tag{3}$$

Where k is the number of clusters, n is the number of classes, p_b is the case b and the pixel with coordinates x and y analyzed, c_a is the centroid of cluster a, and C_k is the objective function that provides a quantized image of k clusters [24].

The number of clusters selected is $k = 2$, since it is desired to separate the region of the blood vessel and biological tissue. There are two ways to select the k points. The first way is to randomly select the k points as cluster centers. The second way is

to choose specific points from the input data. In this work, random values for k point were selected. Then, K-means clustering measures the distance between each of the data and each of the selected points, assigning the closest point. Then, a new group of centroids is randomly selected, and repeat the procedure a certain number of times. The goal of K-means clustering is to search different data sets until the most appropriate one is found. In this work, the number of repetitions made was 20. The analysis is carried out until the same points are assigned to each group in consecutive rounds. That is, results repeated in the consecutive analysis. Increasing the number of iterations for this work does not suggest a significant improvement in the clustering process.

The K-means clustering algorithm has a few features that should be highlighted, it is fast, robust, and simple that provides reliable results when the data sets are different or separated from each other in a linear way. Clustering may not work well if it contains heavily overlapping data or if the data are noisy or full of outliers. In RSI images, it is common to find these outliers, since the nature of the images is noisy or random. Therefore, the use of classical contrast calculation methods, and contrast improvement methods, to generate LSCI images allow K-means clustering to be an efficient segmentation method. Unlike other segmentation methods [17], [19], [20], it relies on the spatial distribution of the contrast values to generate the clusters and not on the histogram distribution, which if not correctly treated, can lead to problems of under-segmentation or over-segmentation.

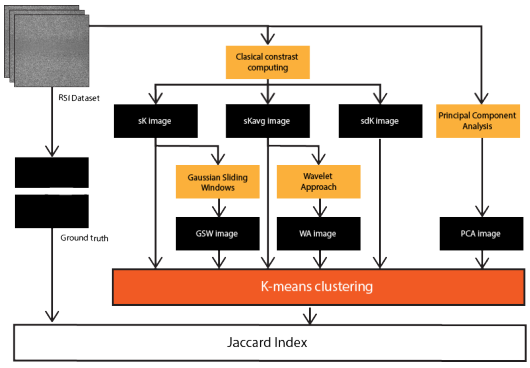

Fig. 3: The workflow of the proposed methodology. The flow starts in the RSI dataset. It then performs different contrast calculations (sK, sK_{avg} and sdK), and applies contrast improvement methods (GSW, WA). Finally, it evaluates the localization performance of K-means clustering.

The workflow is shown in Fig. 3. It can be divided into three important steps. First, the acquisition of RSI images. Second, the contrast calculation through the different methods implemented in this work. Third, the localization of blood vessels using K-means clustering and its obtained performance.

III. RESULTS AND DISCUSSION

A. Visualization of blood vessels

The performance of blood vessel localization depends on the calculation of contrast in RSI images (sK,sK_{avg} and sdK methods) and the contrast improvement in LSCI images (GSW, PCA, and WA methods).

The results obtained from the implementation of the models described in Sec. II-C. Be the RSI column, samples in different depths ($0\mu m$, $190\mu m$, $310\mu m$, $510\mu m$ and $1000\mu m$) of the RSI input images. In RSI column, can be observed that the intensity values of the RSI images from $190\mu m$ depth, it is difficult to establish the boundaries between the blood vessel and the biological tissue. For this reason, methods that calculate contrast are the most used alternative in LSI.

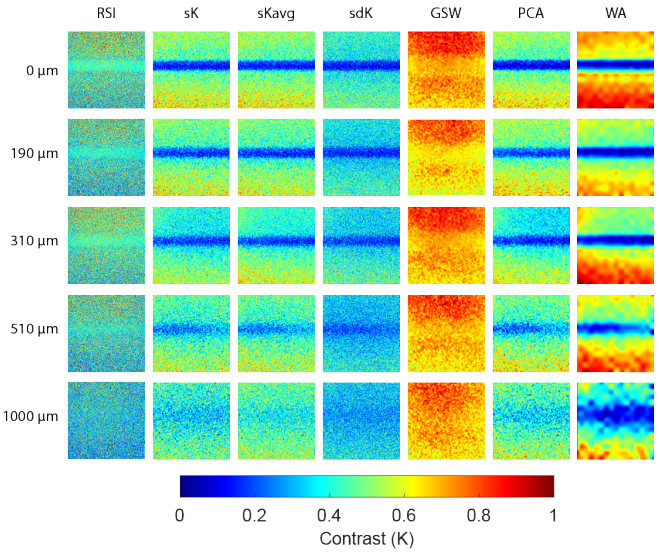

Fig. 4: Calculation results (sK, sK_{avg} and sdK) and contrast improvement (GSW, PCA and WA) for 5 depth levels ($0\mu m$, $190\mu m$, $310\mu m$, $510\mu m$ and $1000\mu m$) in *in-vitro* LSCI images.

The results of the sK and sK_{avg} methods are very similar to each other, especially when the depth of the blood vessel is at $0\mu m$ and $190\mu m$. However, when the following level of depth is analyzed ($310\mu m$) it can be observed that sK begins to lose definition at the edges of the blood vessel. This indicates that sK_{avg} is more efficient than sK in establishing the boundaries between the blood vessel and biological tissue at $310\mu m$ depth. However, although sK_{avg} seems to have better results at $310\mu m$, when analyzing the $510\mu m$ depth level, it does not seem to be different from sK. It could be said that the sK and sK_{avg} methods are limited to the study of blood vessels up to $310\mu m$ depth. The sdK method presents good results in the calculation of contrast at $0\mu m$, $190\mu m$, $310\mu m$ and $510\mu m$ depths. However, it can be observed that from the $0\mu m$ depth, it maintains a greater amount of noise with respect to the sK and sK_{avg} methods. This phenomenon is due to the fact that the contrast calculation is performed using anisotropic windows. In $510\mu m$, the sdK method improves the contrast despite the noise in the image, however, it is difficult to establish the boundaries between the blood vessel and the biological tissue.

The GSW method for the dataset used in this methodology does not present good results for any depth. It is possible that the dimensions of the LSCI images or the level of noise present in the image require parameter adjustment. The PCA method has an advantage over the contrast calculation methods since the filtering is done before the contrast calculation. Compared to the sK, sK_{avg} and sdK methods, it gives good results at $0\mu m$, $190\mu m$, $310\mu m$ and $510\mu m$ depths. In the case of the $510\mu m$ depth, the contrast is improved in the central region of the blood vessel, however, there is no definition of the limits between the blood vessel and the biological tissue. Finally, the sK_{avg}-based WA method shows good results for blood vessels up to $510\mu m$ depth. On the one hand, the limits of the blood vessel are well defined and its contrast values are close to 0. On the other hand, the region of the biological tissue maintains mostly values close to 1.

B. Localization of blood vessels

In the Sec. III-A, the results of the calculation and contrast improvement for the six methods of this methodology are shown. Under the assumption that the pixels are separated into groups defined by the contrast values in the blood vessel (low contrast) and biological tissue regions (high contrast), the K-means clustering method can be implemented.

TABLE I: Results of the methods implemented in this methodology (sK, sK_{avg}, sdK, GSW, PCA and WA) The results are measured with Accuracy (ACC), Precision (PRE), True Positive Rate (TPR), True Negative Rate (TNR), F1-score (F1) and Jaccard Index (JI).

Method	ACC	PRE	TPR	TNR	F1	JI
sK	0.88±0.07	0.61±0.24	0.65±0.18	0.92±0.06	2.61±0.71	0.49±0.22
sK_{avg}	0.89±0.08	0.65±0.25	0.70±0.17	0.93±0.06	0.54±0.23	0.54±0.23
sdK	0.82±0.07	0.42±0.17	0.60±0.16	0.86±0.06	2.40±0.65	0.34±0.15
GSW	0.66±0.08	0.22±0.04	0.54±0.12	0.69±0.10	2.15±0.48	0.18±0.03
PCA	**0.92±0.07**	0.75±0.24	0.75±0.16	**0.95±0.05**	3.00±0.64	**0.63±0.23**
WA	0.85±0.18	**0.85±0.18**	**0.86±0.34**	0.85±0.17	**3.82±0.82**	0.61±0.30

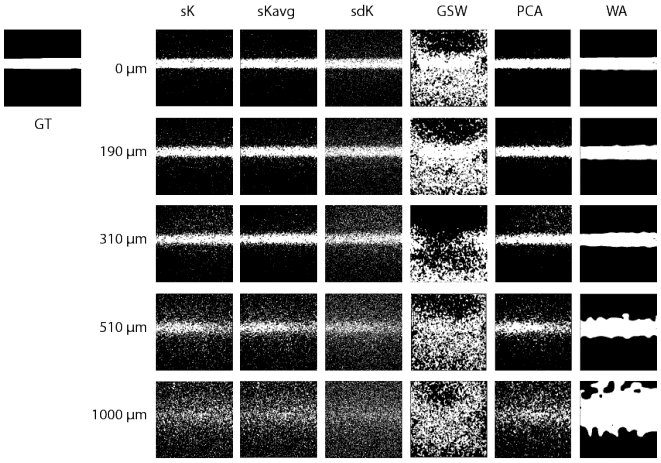

Fig. 5: K-means clustering results for calculation methods (sK, sK_{avg} and sdK) and contrast improvement (GSW, PCA and WA) for 5 depth levels ($0\mu m$, $190\mu m$, $310\mu m$, $510\mu m$ and $1000\mu m$) in *in-vitro* RSI images.

The results obtained from the implementation of the K-means clustering model are presented in Fig. 5. Let GT be the segmentation objective. sK, sK_{avg} and sdK, the results obtained from the contrast calculation methods, and GSW, PCA and WA, contrast improvement, studied for 5 depth levels ($0\mu m$, $190\mu m$, $310\mu m$, $510\mu m$ and $1000\mu m$).

The results of the sK, sK_{avg}, and sdK methods are similar when the blood vessel depth is equal to or less than $310\mu m$. It can be seen that sK_{avg} is the method that has less dispersion of particles around the blood vessel when K-means clustering is implemented since it has a greater definition of the borders between regions. When the depth of the blood vessel increases to $510\mu m$ depth, it is not possible to establish the boundaries between both regions. There is a high amount of scattered particles throughout the image, although most remain in the central region of the image.

In this work it can be established that the classic contrast calculation methods (sK, sK_{avg}, and sdK), are efficient for locating superficial blood vessels ($\rho < 100\mu m$) and some not so deep ($\rho < 300\mu m$). It can be observed that during contrast calculation, LSCI images maintain a large amount of noise and because of this, blood vessel and biological tissue segmentation declines.

Regarding contrast improvement methods, GSW lacks contrast between regions. As a result of implementing K-means clustering in GSW, blood vessel segmentation is poor. On the other hand, PCA presents very favorable results. The localization of blood vessels is efficient at depths such as $510\mu m$, where the main structure of the blood vessel is maintained with some scattering of particles around it. The boundaries between both regions are sufficient to distinguish where the blood vessel begins and where it ends, but not efficient. PCA is a useful method for filtering in RSI images, however, it maintains a moderate amount of noise, which even at $510\mu m$ depth, makes it difficult to establish boundaries. Finally, the WA method presents good results in localizing superficial ($\rho < 100\mu m$) and deep (up to $510\mu m$) blood vessels. It is easy to determine the boundaries between the blood vessel and biological tissue. However, compared to PCA, it has problems of over-segmentation. That is to say, due to the parameters selected during the filtering they present a dilation effect of the blood vessel. It can be assumed that by optimizing the filtering and clustering parameters, better results can be obtained, even in deep vessels such as $1000\mu m$.

An objective way to establish the results of blood vessel location is through a similarity metric between clusters. Table I summarizes the results of the full dataset by combining the depths ($0\mu m < \rho < 1000\mu m$). Also, the localization results are shown with different evaluation metrics: Accuracy (ACC), Precision (PRE), True Positive Rate (TPR), True Negative Rate (TNR), F1-score (F1) and Jaccard Index (JI).

The results suggest that PCA and WA have the best performance in location with K-means clustering, according to the selected metrics. On one hand PCA presents the best results with ACC (0.92±0.07), TNR (0.95±0.05) and JI (0.63±023). On the other hand, WA has the best results when evaluated with PRE (0.85±0.18), TPR (0.86±0.34) and F1 (3.83±0.82).

To describe in detail the results obtained from the K-means clustering method for the contrast models, hereafter the JI metric is used (Fig. 6). Given two binary images A (segmentation) and B (ground truth), JI is defined as $JI(A,B) = TP/TP + FP + FN$, where, TP are True Positives, FP are False Positives and FN are False Negatives.

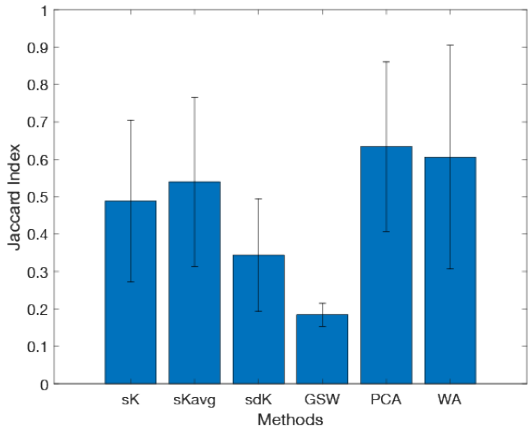

Fig. 6: Localization results for the dataset with the methods sK, sK_{avg}, sdK, GSW, PCA and WA. The measurement was performed with Jaccard index (JI).

Contrast calculation methods such as sK and sK_{avg} have favorable results for the entire dataset. As can be seen in the visualization and localization sections, the methods follow a similar behavior, where sK_{avg} (0.54±0.23) is superior to sK (0.49±0.22) by a very short difference. The mean and standard deviation values are

similar. However, the *sdK* method, presents a lower performance for contrast calculation methods (0.34 ± 0.15), as described in the Sec. III-A this effect is because the *sdK* method is not very efficient in reducing noise, therefore, K-means clustering is unable to correctly cluster blood vessel and biological tissue.

In contrast improvement methods, PCA (0.63 ± 0.23) and WA have the best results of the implemented methods. PCA has the best performance due to having a higher mean value and a lower standard deviation value, compared to WA (0.61 ± 0.30). The results suggest that the use of K-means clustering for PCA and WA contrast improvement methods can localize superficial and deep blood vessels. This implies that segmenting LSCI images with the K-means clustering method when the amount of noise is low and the regions are well contrasted increases the performance for most depths.

IV. CONCLUSIONS

In Laser Speckle Contrast Imaging, the visualization and localization is an important task in determining the presence of blood vessels inside the biological tissue. However, Laser Speckle Contrast Imaging have some drawbacks when the depth of the blood vessels increases. In the present work, the K-means clustering method was used to segment *in-vitro* RSI and *in-vitro* LSCI images automatically at different depth levels. In this study different methods to calculate and improve contrast were implemented. LSCI images obtained from contrast improve methods such as PCA and WA show high performance (even in deep blood vessels).

It was observed that the most relevant aspects in the K-means clustering process are related to the filtering processes that reduce contrast outliers in LSCI images, and improve contrast between blood vessel and biological tissue regions. Also, reducing the fusion of regions during contrast calculation increases the ability to discriminate between blood vessel and biological tissue. Finally, the experiments performed establish that the segmentation of blood vessels in LSCI images *in-vitro* depends on contrast computation methods that separate blood vessels from biological tissue. Therefore, developing methods that allow contrast improvement in noisy images such as LSCI is an expanding field of research.

REFERENCES

[1] A. Y. Neganova, D. D. Postnov, O. Sosnovtseva, J. C. B. Jacobsen, "Rat retinal vasomotion assessed by laser speckle imaging". *PloS one*, vol. 12, no. 3, pp. e0173805, 2016.

[2] A. Cho, C. Yeon, D. Kim, and E. Chung. "Laser speckle contrast imaging for measuring cerebral blood flow changes caused by electrical sensory stimulation". *Journal of the Optical Society of Korea*, vol. 20, no. 1, pp. 88-93, 2016.

[3] W. J. Moy, G. Ma, K. M. Kelly and B. Choi, "Hemoporin-mediated photodynamic therapy on normal vasculature: implications". *Journal of clinical and translational research*, vol. 2, no. 3, pp. 107, 2016.

[4] D. A. Boas, and A. K. Dunn, "Laser speckle contrast imaging in biomedical optics". *Journal of biomedical optics*, vol. 15, no. 1, pp. 011109, 2010.

[5] D. Briers, D. Duncan, S. Kirkpatrick, M. Larsson, T. Stromberg, and O. Thompson, "Laser speckle contrast imaging: Theoretical and practical limitations". *Journal of biomedical optics*, vol. 18, no. 6, pp. 1–9, 2013.

[6] Y. A. Aizu and T. Asakura, "Bio-speckle phenomena and their application to the evaluation of blood flow". *Optics & Laser Technology*, vol 23, no. 4, pp. 205–219, 1991.

[7] M. Draijer, E. Hondebrink, T. van Leeuwen, and W. Steenbergen. "Review of laser speckle contrast techniques for visualizing tissue perfusion". *Lasers in medical science*, vol 24, no. 6, pp. 639, 2019.

[8] D. D. Duncan and S. J. Kirkpatrick, "Can laser speckle flowmetry be made a quantitative tool?". *Journal of the Optical Society of America*, vol. 25, no. 8, pp. 2088–2094, Aug. 2008.

[9] P. G. Vaz, A. Humeau-Heurtier, E. Figueiras, C. Correia, and J. Cardoso. "Laser speckle imaging to monitor microvascular". *IEEE reviews in biomedical engineering*, vol. 9, pp. 106–120, 2016.

[10] C. Perez-Corona, H. Peregrina-Barreto, J. Rangel-Magdaleno, R. Ramos-Garcia, and J. Ramirez-San-Juan, "Spacedirectional laser speckle contrast imaging to improve blood vessels visualization". *In 2018 IEEE International Instrumentation and Measurement Technology Conference (I2MTC)* pp. 1-5, May, 2018.

[11] K. Basak, G. Dey, M. Mahadevappa, M. Mandal, and P. K. Dutta, "In vivo laser speckle imaging by adaptive contrast computation for microvasculature assessment". *Optics and Lasers in Engineering*, vol. 62, pp. 87-94, 2014.

[12] A. Rege, J. Senarathna, N. Li, and N. V. Thakor, "Anisotropic processing of laser speckle images improves spatiotemporal resolution". *IEEE Transactions on Biomedical Engineerin*, vol. 59, no. 5, pp. 1272-1280, 2012.

[13] H. Peregrina-Barreto, E. Perez-Corona, J. Rangel-Magdaleno, R. Ramos-Garcia, R. Chiu and J. C. Ramirez-San-Juan, "Use of kurtosis for locating deep blood vessels in raw speckle imaging using a homogeneity representation". *Journal of biomedical optics*, vol. 22, no. 6, pp. 066004, 2017.

[14] S. A. Rosales-Nunez, H. Peregrina-Barreto, J. Rangel-Magdaleno, R. J. Ramirez-San-Juan, and I. Terol-Villalobos, "Automatic scale determination for adaptive windowing in Laser Speckle Imaging", *In 2018 IEEE International Instrumentation and Measurement Technology Conference (I2MTC)* pp. 1-5, May, 2018.

[15] E. B. Postnikov, M. O. Tsoy, and D. E. Postnov, "Matlab for laser speckle contrast analysis (lasca): a practice-based approach". *Saratov Fall Meeting 2017: Laser Physics and Photonics XVIII; and Computational Biophysics and Analysis of Biomedical Data IV. International Society for Optics and Photonics*, vol. 10717, pp. 1071728, 2018.

[16] J. A. Arias-Cruz, R. Chiu, H. Peregrina-Barreto, R. Ramos-Garcia, T. Spezzia-Mazzocco, and J. C. Ramirez-San-Juan, "Visualization of in vitro deep blood vessels using principal component analysis based laser speckle imaging. *Biomedical optics express*, vol. 10, no. 4 pp. 2020-2031, 2019.

[17] E. Morales-Vargas, J. Sosa-Martinez, H. Peregrina-Barreto, J. Rangel-Magdaleno and J. C. Ramirez-San-Juan, "A morphological approach for locating blood vessels in laser contrast speckle imaging". *In 2018 IEEE International Instrumentation and Measurement Technology Conference (I2MTC)*, pp. 1-6, May, 2018.

[18] E. Morales-Vargas, H. Peregrina-Barreto, J. Rangel-Magdaleno and J. C. Ramirez-San-Juan, "Estimation of blood vessels diameter by region growing in laser speckle contrast imaging". *In 2019 IEEE International Instrumentation and Measurement Technology Conference (I2MTC)* pp. 1-5, May, 2019.

[19] F. Lopez-Tiro, H. Peregrina-Barreto, J. Rangel-Magdaleno and J. C. Ramirez-San-Juan, "Visualization of in-vitro Blood Vessels in Contrast Images Based on Discrete Wavelet Transform Decomposition". *In 2019 IEEE International Instrumentation and Measurement Technology Conference (I2MTC)* pp. 1-6, May, 2019.

[20] F. Lopez-Tiro, H. Peregrina-Barreto, J. Rangel-Magdaleno, J.C. Ramirez-San-Juan, and J.M. Ramirez-Cortes, "Effect of the Exposure Time in Laser Speckle Imaging for Improving Blood Vessels Localization: a Wavelet Approach". *In 2020 IEEE International Instrumentation and Measurement Technology Conference (I2MTC)* pp. 1-6, May, 2020.

[21] D. D. Postnov, V. V. Tuchin, and O. Sosnovtseva, "Estimation of vessel diameter and blood flow dynamics from laser speckle images. *Biomedical optics express*, vol. 7, no. 7, pp. 2759-2768, 2016.

[22] E. B. Postnov, M. O. Tsoy, P. A. Timoshina, and D. E. Postnov, "Gaussian sliding window for robust processing laser speckle contrast images". *International journal for numerical methods in biomedical engineering*, vol. 34, no. 4,e3186, 2019.

[23] R. B. Saager, C. Kondru, K. Au, K. Sry, F. Ayers, and A. J. Durkin, "Multilayer silicone phantoms for the evaluation of quantitative optical techniques in skin imaging". *International Society for Optics and Photonics*, vol. 7567, pp. 756-706, 2010.

[24] N. Dhanachandra, K. Manglem and Y. J. Chanu. "Image segmentation using K-means clustering algorithm and subtractive clustering algorithm". *Procedia Computer Science*, vol. 54, pp. 764-771, 2015.